



ChemComm

**Lanthanide-based luminescent probes for biological magnesium: accessing polyphosphate-bound Mg<sup>2+</sup>**

Journal:	<i>ChemComm</i>
Manuscript ID	CC-COM-12-2022-007095
Article Type:	Communication

SCHOLARONE™  
Manuscripts

## COMMUNICATION

Lanthanide-based luminescent probes for biological magnesium: accessing polyphosphate-bound  $Mg^{2+}$ 

Received 00th January 20xx,  
Accepted 00th January 20xx

Brismar Pinto-Pacheco,<sup>a</sup> Qitian Lin,<sup>a</sup> Claudia W. Yan,<sup>a</sup> Symara de Melo Silva,<sup>a</sup> and Daniela Buccella<sup>\*a</sup>

DOI: 10.1039/x0xx00000x

**Biomolecule-bound  $Mg^{2+}$  species, particularly polyphosphate complexes, represent a large and dynamic fraction of the total cellular magnesium that is essential for cellular function but remains invisible to most indicators. Here we report a new family of Eu(III)-based indicators, the MagQEu family, functionalized with a 4-oxo-4H-quinolizine-3-carboxylic acid metal recognition group/sensitization antenna for turn-on, luminescence-based detection of biologically relevant  $Mg^{2+}$  species.**

Magnesium(II) ions are required for all central cellular functions, including protein synthesis, cell division, metabolism and modulation of ion transport.<sup>1</sup> Disrupted homeostasis of this metal has been linked to pathologies ranging from cancer to neurodegeneration.<sup>1b,2</sup> Cellular levels of  $Mg^{2+}$  are maintained typically within 16 - 20 mM in mammalian cells. Only a small fraction (~5%) of the total  $Mg^{2+}$  is in “free” form, whereas the largest pool of  $Mg^{2+}$  is tightly bound to biomolecules such as polyphosphates and proteins.<sup>2a</sup> This “bound” pool, especially polyphosphates such as MgATP, is highly dynamic and its concentration and speciation can change rapidly. The ability to track it in real time is thus of great importance.

Spectroscopic and imaging techniques based on luminescent indicators are ubiquitous tools in the dynamic study of metal ions, including  $Mg^{2+}$ , in live cells and tissues.<sup>3</sup> Most available indicators, however, only access the readily exchangeable or free metal pool (Figure 1A)<sup>2c,4</sup> and offer little to no information on the tightly biomolecule-chelated fraction. In an effort to address this limitation, Wolf and co-workers developed the DCHQ series of indicators<sup>5</sup> that bind  $Mg^{2+}$  tightly, outcompeting endogenous chelators and stripping them of the metal (Figure 1B). This competition accesses most, if not all,  $Mg^{2+}$ -containing complexes but disrupts the natural speciation of the metal in the cell. Direct, non-disruptive probing of biomolecule-bound  $Mg^{2+}$  in intact cells remains a challenge.

Seeking an alternative strategy, we focused on 4-oxo-4H-quinolizine-3-carboxylic acid (Figure 2A) as  $Mg^{2+}$ -selective binding moiety.<sup>6</sup> Previous studies from our group revealed that

this bidentate chelator allows the formation of ternary indicator- $Mg^{2+}$ -ATP species.<sup>7</sup> In this report, we describe the development of Eu(III)-based luminescent probes that capitalize on the formation of such ternary complexes to enable ‘turn-on’ detection of polyphosphate-bound  $Mg^{2+}$ , taking an important step toward enabling real-time monitoring of total cellular  $Mg^{2+}$  by optical techniques.

#### MagQEu1: a luminescent sensor for biomolecule-bound $Mg^{2+}$

We envisioned a design in which the 4-oxo-4H-quinolizine-3-carboxylic acid moiety would function as sensitizing antenna for an Eu(III) complex, modulating the emission of the lanthanide in response to the binding of  $Mg^{2+}$  in various biologically relevant complexes (Figure 2). A triazole connects the antenna and the luminophore, bringing them within distance to enable energy transfer. The chosen quinolizine acid displays properties that seemed well suited for the dual binding moiety/antenna role. First, it can recognize  $Mg^{2+}$  in various coordination environments, as illustrated by similar dissociation constants for the 1:1 complex with  $Mg^{2+}$  ( $K_d = 1.55$  mM) and for the

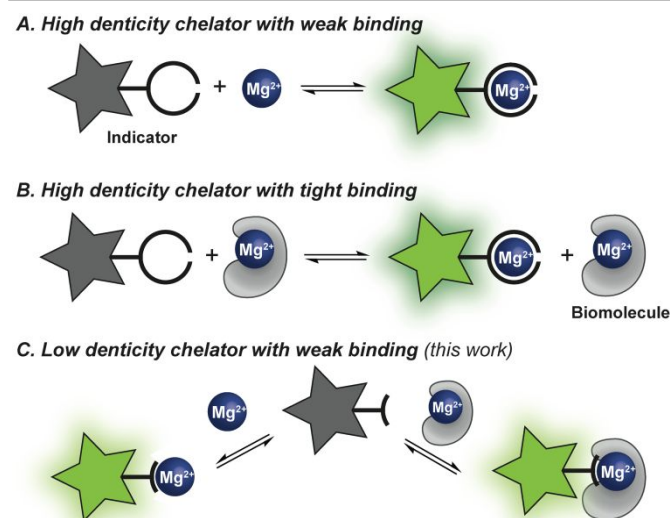


**Figure 1.** Types of  $Mg^{2+}$  indicators. (A) Weak binders with high density probe the ‘free’ or labile  $Mg^{2+}$  ion pool, whereas (B) tight binders with high density outcompete endogenous chelators and access the biomolecule-bound pool. (C) Our proposed design based on a weak binder of low density samples both free and biomolecule-bound  $Mg^{2+}$  through the formation of ternary complexes, without disrupting natural  $Mg^{2+}$  speciation.

<sup>a</sup> Department of Chemistry, New York University, 100 Washington Square East, New York, NY 10003.

Electronic Supplementary Information (ESI) available: Additional spectra, experimental details and data for characterization of new compounds. See DOI: 10.1039/x0xx00000x

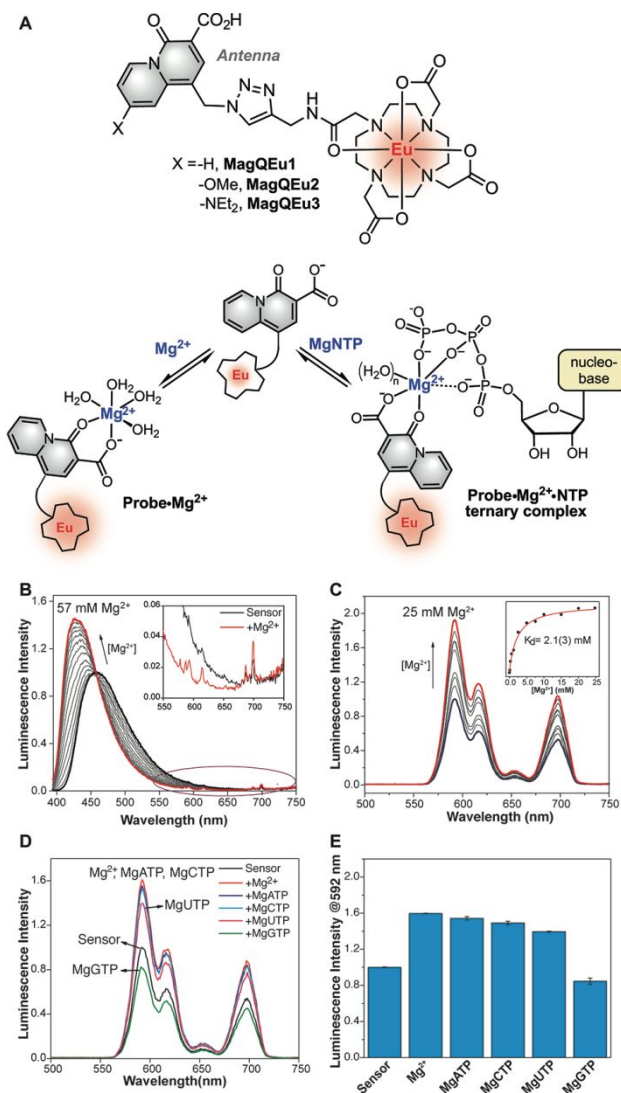


**Figure 2.** (A) Structure and proposed detection scheme of **MagQEu** sensors. (B) Steady-state and (C) time-gated luminescence spectra of **MagQEu1** in response to increasing concentrations of  $Mg^{2+}$ . (D) Time-gated luminescence spectra and (E) time-gated luminescence intensity at 592 nm in response to 5 mM of various MgNTPs. Averages of triplicate measurements. All measurements conducted with 5  $\mu M$  **MagQEu1** in aqueous buffer (50 mM PIPES, 100 mM KCl, pH 7.0) at 25 °C. Excitation wavelength  $\lambda_{exc}$  392 = nm. Delayed detection: 0.1 ms, integration 1 ms.

ternary complex with MgATP ( $K_d = 1.81$  mM).<sup>7</sup> Second, it displays an absorption maximum at 385 nm,<sup>6a</sup> meeting the minimum energy requirements for effective sensitization of Eu(III).<sup>8</sup> Third, a shift in the emission spectrum indicates that the energy levels are modulated by coordination of  $Mg^{2+}$ , suggesting the possibility of engineering metal-dependent

changes in sensitization. The new sensor, **MagQEu1**, was prepared by copper(I)-catalyzed cycloaddition of the azide-containing antenna **4a** and an alkyne-decorated Eu cyclen complex<sup>9</sup> (Scheme S1) followed by quantitative hydrolysis of the quinolizine ester.

The properties of **MagQEu1** were first evaluated by steady-state luminescence experiments in aqueous buffer at pH 7.0, exciting at the absorption maximum of the quinolizine (Table 1 and Figure S1, Supporting Information). The indicator displays the expected narrow emission peaks in the range of 580–700 nm (Figure 2B) corresponding to Eu(III) luminescence.<sup>10</sup> Residual fluorescence from the antenna is observed at 458 nm. Treatment with increasing concentrations of  $Mg^{2+}$  induces a blue shift and small enhancement in the emission of the antenna, concomitant with a marked increase in the luminescence intensity from the lanthanide (Figures 2B,C). Lifetime measurements in deuterated buffers indicate that the number of Eu-coordinated water molecules,  $q$ , is one and remains the same for the  $Mg^{2+}$ -bound and free sensors (Table S1), thus the enhancement can be attributed to modulation of the energy of the antenna by  $Mg^{2+}$  binding.

The short-lived background signal of the antenna is easily removed by detection after a 0.1 ms delay (Figure 2C). Non-linear fit of the time-gated luminescence at 592 nm as a function of  $Mg^{2+}$  concentration (Figure S2) results in an apparent dissociation constant  $K_d = 2.1 \pm 0.3$  mM for the binary **MagQEu1**- $Mg^{2+}$  complex. This  $K_d$  renders the sensor sensitive to physiological concentrations of free  $Mg^{2+}$ , and it is unlikely to result in displacement of common endogenous  $Mg^{2+}$  chelators such as ATP or other polyphosphates, which have dissociation constants for  $Mg^{2+}$  in the micromolar range.<sup>11</sup>

Given that complexes with nucleoside triphosphates (NTPs) comprise a large fraction of the bound pool of cellular  $Mg^{2+}$ ,<sup>12</sup> we evaluated the changes in the emission profile of **MagQEu1** upon exposure to MgATP, MgCTP, MgUTP and MgGTP. The intensity of the Eu(III)-based luminescence increased upon treatment with the various complexes, with the exception of MgGTP (Figure 2D, E and S3). Metal-free triphosphates, including ATP, CTP and UTP, did not induce any changes in the spectroscopic properties of **MagQEu1** under similar conditions (Figure S4), thus confirming that the observed luminescence enhancement depends on the coordination of the antenna to the  $Mg^{2+}$  center. Non-linear fit of luminescence at 592 nm was used to determine the dissociation constants from the various MgNTP complexes based on a 1:1 complex-to-indicator binding model (Table 1 and Figure S5). All  $K_d$  values are in the low millimolar range, close to physiological concentrations of

**Table 1.** Photophysical properties and apparent dissociation constants of **MagQEu1-3** in the presence of  $Mg^{2+}$  and MgNTP complexes.<sup>a</sup>

Compound	$\lambda_{exc}$ (nm)		$K_d$ (mM) <sup>b</sup>						pKa
	Free	$Mg^{2+}$ -bound <sup>c</sup>	$Mg^{2+}$	MgATP	MgCTP	MgGTP	MgTTP	MgUTP	
<b>MagQEu1</b>	392	392	2.1(3)	2.6(6)	2.1(4)	N.D.	N.D.	1.7(9)	5.46(8)
<b>MagQEu2</b>	388	381	1.08(1)	1.37(2)	2.3(6)	N.D.	N.D.	2.5(2)	6.44(4)
<b>MagQEu3</b>	395	391	0.93(5)	0.49(7)	0.57(3)	0.39(5)	0.47(6)	0.4(2)	6.92(8)

<sup>a</sup>All measurements performed at a probe concentration of 5  $\mu M$  in aqueous buffer (50 mM PIPES, 100 mM KCl) at pH 7, 25 °C except pH titrations. N.D. = Not Determined. Numbers in parenthesis represent the uncertainty in the last significant figure, calculated from the standard deviation of triplicate measurements. <sup>b</sup> $K_d$  values reported for the MgNTPs correspond to the equilibrium constants for the reaction  $[Sensor.MgNTP] = Sensor + MgNTP$ . <sup>c</sup>At saturating concentration of  $Mg^{2+}$ .

MgNTPs,<sup>13</sup> thus suggesting our indicator design is a good starting point for probing relevant biomolecule-bound Mg<sup>2+</sup> species.

The lack of Eu(III) luminescence enhancement observed with MgGTP, however, forecasts possible limitations in the application of **MagQEu1** for evaluating changes of biomolecule-Mg<sup>2+</sup> levels in guanine-rich samples. Given that guanine is a readily oxidizable base, we hypothesized that the luminescence turn-off of **MagQEu1** in the presence of MgGTP could be the result of PeT from the guanine to the antenna in a ternary **MagQEu1**-Mg<sup>2+</sup>-GTP complex. A decrease in the residual fluorescence emission of the antenna in the presence of MgGTP (Figure S3), which is not observed upon treatment of the sensor with other MgNTPs, is consistent with this notion, as it reveals the effects of a fast non-radiative decay process.

#### Design of **MagQEu2** and **MagQEu3**: circumventing PeT quenching of the antenna with nucleobases

Non-radiative decay based on PeT could be rendered less competitive by tuning the redox properties of the antenna to disfavor its photoreduction. To this end, we modified the quinolizine moiety of the indicator to include electron donating groups at the 8 position (Scheme S1).<sup>6a</sup> The electrochemical properties of the substituted quinolizines were determined by cyclic voltammetry in acetonitrile and compared against the parent, unsubstituted antenna. The reduction potential of all the compounds and the driving force for PeT with various nucleobases, calculated using the Rehm-Weller equation,<sup>14</sup> are summarized in Tables S2 and S3, respectively. As anticipated, the reduction potential for the quinolizine increases significantly upon substitution with strong electron donating groups, making photoreduction unfavorable. In contrast, PeT with guanine is predicted to be favorable for the unsubstituted antenna, consistent with the luminescence quenching effect observed for **MagQEu1** in the presence of MgGTP.

Encouraged by the results of the electrochemical studies, we pursued the synthesis of Eu(III)-based indicators **MagQEu2** and **MagQEu3** (Schemes S1, S2). Their photophysical properties were characterized by steady-state and time-gated luminescence measurements in aqueous buffer (Figures S6-S8), with excitation at the absorption maximum of the corresponding antenna. Upon treatment with increasing concentrations of Mg<sup>2+</sup> in aqueous buffer, strong luminescence enhancement was observed (Figure S6). Residual fluorescence from the antenna is still observed for all sensors; for example, comparison of the emission at 408 nm from **MagQEu3** versus that from a concentration-matched sample of quinolizine **7c** (Scheme S2) reveals a 33% decrease in intensity caused by the proximity of the lanthanide. This modest decrease suggests limited deactivation of the antenna's excited state by PeT to the Eu<sup>3+</sup> center, which can also quench sensitized lanthanide emission.<sup>15</sup>

Time-gated luminescence experiments for **MagQEu2** in the presence of MgNTPs showed a luminescence enhancement with Mg<sup>2+</sup> complexes of ATP, CTP and UTP, but a small decrease with MgGTP (Figure 3A,B). In contrast, **MagQEu3** exhibited a luminescence enhancement with all MgNTP complexes tested,

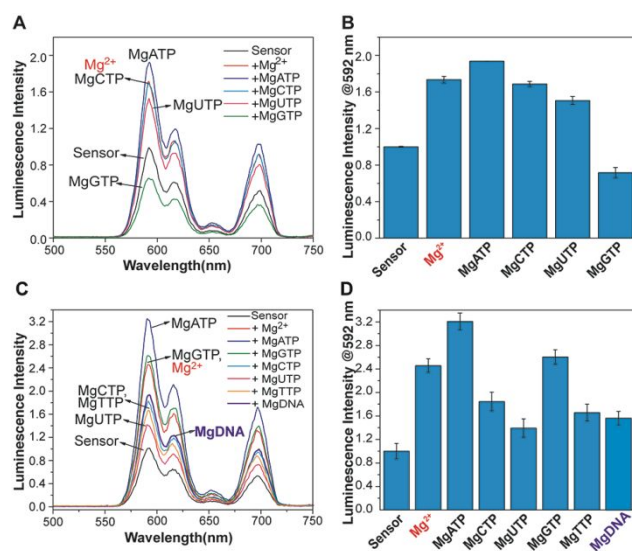


**Figure 3.** Time gated luminescence of **MagQEu2** (A, B) and **MagQEu3** (C, D) in the presence of Mg<sup>2+</sup> containing species. (A, C) Time gated Luminescence spectrum and (B, D) luminescence intensity at 592 nm; averages of triplicate measurements. Conditions: 5  $\mu$ M sensor treated with MgCl<sub>2</sub> or Mg<sup>2+</sup> complex (5 mM in Mg<sup>2+</sup>, [Mg]/[P] = 0.5 for MgDNA), in 50 mM PIPES, 100 mM KCl, pH 7.0, 25  $^{\circ}$ C. Excitation wavelength  $\lambda_{exc}$ =388 nm for **MagQEu2** and  $\lambda_{exc}$ =395 nm **MagQEu3**. Delayed detection: 0.1 ms.

including MgGTP and MgTTP (Figure 3C,D). These results are consistent with our design hypothesis and support the notion that the diethylamino substituent shifts the reduction potential of the antenna enough to prevent photoreduction by the guanine base. Control experiments conducted with 5 mM of each NTP in the absence of Mg<sup>2+</sup> (Figures S9 and S10) did not reveal major changes in luminescence, indicating that the observed enhancement still relies on the coordination of the antenna to Mg<sup>2+</sup>.

The apparent dissociation constants for Mg<sup>2+</sup> and for MgNTPs determined from time-gated luminescence experiments (Figures S11 and S12) are summarized in Table 1. They are similar for the various MgNTPs and well aligned with typical concentrations in the cell.<sup>13</sup> Overall, they are slightly lower for **MagQEu2** and **-3** than for **MagQEu1**. This small change is a consequence of the electron-donating effect of ethoxy and diethylamino substituents, which make the quinolizine acid a stronger chelator. The effect is also reflected on the pK<sub>a</sub> (Table 1, Figure S13), which increases from **MagQEu1** to **MagQEu2** and **-3**. The apparent dissociation constants, in combination with the capability of detecting Mg<sup>2+</sup> in guanine-rich samples, makes **MagQEu3** the best candidate for probing biological bound Mg<sup>2+</sup> in cellular matrices and biological samples.

Magnesium(II) is a natural counterion of DNA, and complexation of the metal cation to its phosphate backbone plays an important role in genomic stability.<sup>16</sup> To investigate whether the **MagQEu** family can access this important pool of biomolecule-bound Mg<sup>2+</sup>, luminescence data of the sensors was recorded in the presence of Mg<sup>2+</sup>-bound DNA at a [Mg<sup>2+</sup>]/[phosphate]=0.5.<sup>17</sup> As anticipated from the results with the MgNTPs, neither **MagQEu1** nor **MagQEu2** showed a large response to MgDNA (Figures S14 and S15). **MagQEu3**, on the other hand, showed a good luminescence enhancement (Figure

3E,F), though smaller than the enhancement obtained in the detection of free  $Mg^{2+}$ . Future efforts will be devoted to increasing the overall luminescence enhancement for all species by adjusting the antenna-Eu distance and further tuning the antenna electronics to enhance sensitization and possibly diminish nucleobase-dependent differences in response. Despite the limited dynamic range, however, the large changes in luminescence lifetime (Table S1) may offer alternative avenues for application of these sensors in the study of samples undergoing smaller changes.

Time-gated detection makes the long-lived lanthanide luminescence readily discernible from the short-lived fluorescence signal of typical sensors for free  $Mg^{2+}$ ,<sup>4a,4c,18</sup> thus enabling their concurrent use. To illustrate this point, we tested the detection of magnesium in mixtures with different ratios of  $Mg^{2+}$  and MgATP using a combination of **MagQEu3** and **MagB2**, a pentadentate, red-emitting indicator responsive to free  $Mg^{2+}$  (Fig. 4).<sup>4c</sup> As expected, **MagB2** fluorescence emission turned on in the presence of free  $Mg^{2+}$ , whereas **MagQEu3** luminescence responded to all species. The partial turn-on observed for **MagB2** in the presence of MgATP can be attributed to detection of free  $Mg^{2+}$  arising from dissociation of the MgATP complex. We envision that, in combination, analysis of short and long-lived luminescence may afford a more complete and dynamic picture of magnesium speciation in the cell, critical to the study of basic homeostasis mechanisms for this important metal.

In summary, we have developed luminescent, turn-on indicators that offer a new means to probe polyphosphate-bound  $Mg^{2+}$  through formation of ternary complexes. These represent an important step toward dynamic, non-destructive monitoring of total  $Mg^{2+}$  cellular content by optical techniques.

This work was supported in part by the National Science Foundation under grant CHE-1555116, and by the National Institutes of Health under award number R01CA127817. B.P.-P. thanks the NSF for a Graduate Research Fellowship under Grant No. DGE1342536. The authors thank Prof. Michael Ward for access to electrochemistry equipment, Prof. Eray Aydil and Iver Cleveland for assistance with lifetime measurements, and

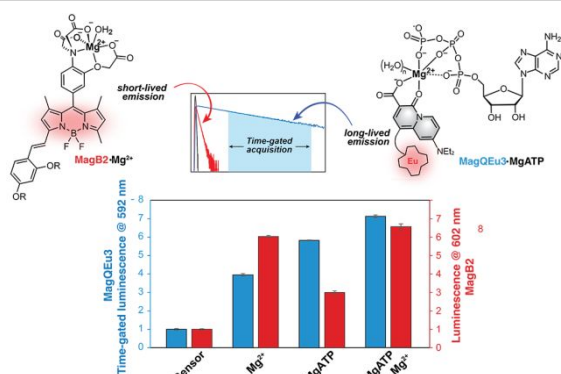


**Figure 4.** Normalized luminescence and time-gated luminescence of an equimolar mixture of **MagQEu3** and **MagB2** in the presence of  $Mg^{2+}$  containing species. Conditions: 5  $\mu$ M of each sensor treated with either 5 mM  $MgCl_2$ , 5 mM MgATP, or 5 mM  $MgCl_2$  + 5 mM MgATP in aqueous buffer pH 7.0.  $\lambda_{exc}$ =395 nm,  $\lambda_{em}$ =592 nm, delayed detection 0.1 ms (blue bars) and  $\lambda_{exc}$ =575,  $\lambda_{exc}$ =602 nm (red bars).

Sophie Lozowski for valuable discussions.

## Conflicts of Interest

There are no conflicts to declare

## Notes and references

- (a) *The Biological Chemistry of Magnesium*, VCH Publishers, Inc, New York, 1995; (b) J. H. F. de Baaij, J. G. J. Hoenderop and R. J. M. Bindels, *Physiol. Rev.*, 2015, **95**, 1.
- (a) A. M. P. Romani, *Magnesium Homeostasis in Mammalian Cells*, Springer, Dordrecht, 2013; (b) J. Ayuk and N. J. L. Gittoes, *Ann. Clin. Biochem.*, 2014, **51**, 179; (c) J. Simón, N. Goikoetxea-Usandizaga, M. Serrano-Maciá, D. Fernández-Ramos, D. Sáenz de Urturi, J. J. Gruskos, P. Fernández-Tussy, S. Lachiondo-Ortega, I. González-Recio, R. Rodríguez-Agudo, et al., *J. Hepatol.*, 2021, **75**, 34.
- (a) K. P. Carter, A. M. Young and A. E. Palmer, *Chem. Rev.*, 2014, **114**, 4564; (b) J. Yin, Y. Hu and J. Yoon, *Chem. Soc. Rev.*, 2015, **44**, 4619.
- (a) M. Liu, X. Yu, M. Li, N. Liao, A. Bi, Y. Jiang, S. Liu, Z. Gong and W. Zeng, *RSC Advances*, 2018, **8**, 12573; (b) T. S. Lazarou and D. Buccella, *Curr. Opin. Chem. Biol.*, 2020, **57**, 27; (c) Q. Lin, J. J. Gruskos and D. Buccella, *Org. Biomol. Chem.*, 2016, **14**, 11381.
- (a) G. Farruggia, S. Iotti, L. Prodi, M. Montalti, N. Zaccheroni, P. B. Savage, V. Trapani, P. Sale and F. I. Wolf, *J. Am. Chem. Soc.*, 2006, **128**, 344; (b) A. Sargenti, G. Farruggia, N. Zaccheroni, C. Marraccini, M. Sgarzi, C. Cappadone, E. Malucelli, A. Procopio, L. Prodi, M. Lombardo, et al., *Nat. Protoc.*, 2017, **12**, 461.
- (a) P. A. Otten, R. E. London and L. A. Levy, *Bioconj. Chem.*, 2001, **12**, 203; (b) H. Komatsu, N. Iwasawa, D. Citterio, Y. Suzuki, T. Kubota, K. Tokuno, Y. Kitamura, K. Oka and K. Suzuki, *J. Am. Chem. Soc.*, 2004, **126**, 16353; (c) Y. Shindo, T. Fujii, H. Komatsu, D. Citterio, K. Hotta, K. Suzuki and K. Oka, *PLoS One*, 2011, **6**, e23684; (d) O. Murata, Y. Shindo, Y. Ikeda, N. Iwasawa, D. Citterio, K. Oka and Y. Hiruta, *Anal. Chem.*, 2020, **92**, 966.
- S. C. Schwartz, B. Pinto-Pacheco, J.-P. Pitteloud and D. Buccella, *Inorg. Chem.*, 2014, **53**, 3204.
- R. A. Poole, G. Bobba, M. J. Cann, J.-C. Frias, D. Parker and R. D. Peacock, *Org. Biomol. Chem.*, 2005, **3**, 1013.
- R. F. H. Viguier and A. N. Hulme, *J. Am. Chem. Soc.*, 2006, **128**, 11370.
- M. C. Heffern, L. M. Matosziuk and T. J. Meade, *Chem. Rev.*, 2014, **114**, 4496.
- (a) C. M. Frey and J. E. Stuehr, *J. Am. Chem. Soc.*, 1972, **94**, 8898; (b) J. C. Sari and J. P. Belaich, *J. Am. Chem. Soc.*, 1973, **95**, 7491.
- A. M. P. Romani, *Arch. Biochem. Biophys.*, 2011, **512**, 1.
- J. O. Park, S. A. Rubin, Y.-F. Xu, D. Amador-Noguez, J. Fan, T. Shlomi and J. D. Rabinowitz, *Nat. Chem. Biol.*, 2016, **12**, 482.
- D. Rehm and A. Weller, *Isr. J. Chem.*, 1970, **8**, 259.
- D. Kovacs and K. E. Borbas, *Coord. Chem. Rev.*, 2018, **364**, 1.
- A. Hartwig, *Mutation Research/Fundamental and Molecular Mechanisms of Mutagenesis*, 2001, **475**, 113.
- K. Serec, S. D. Babić, R. Podgornik and S. Tomić, *Nucleic Acids Res.*, 2016, **44**, 8456.
- (a) V. Trapani, G. Farruggia, C. Marraccini, S. Iotti, A. Cittadini and F. I. Wolf, *Analyst*, 2010, **135**, 1855; (b) M. S. Afzal, J.-P. Pitteloud and D. Buccella, *Chem. Commun.*, 2014, **50**, 11358; (c) G. Zhang, J. J. Gruskos, M. S. Afzal and D. Buccella, *Chem. Sci.*, 2015, **6**, 6841.